cigre Turkey

TEPES
TURKISH JOURNAL OF ELECTRICAL POWER AND ENERGY SYSTEMS

TEPES, Vol. 4, Issue. 1, 2-12, 2024 **DOI:** 10.5152/tepes.2024.23024

RESEARCH ARTICLE

Modeling and Simulation of a Series and Parallel Battery Pack Model in MATLAB/Simulink

Azemtsop Manfo Theodore, Mustafa Ergin Şahin

Department of Electrical and Electronic Engineering, Recep Tayyip Erdoğan University, Rize, Turkey

Cite this article as: A. M. Theodore and M. E. Şahin, "Modeling and simulation of a series and parallel battery pack model in MATLAB/simulink," *Turk J Electr Power Energy Syst.*, 2024; 4(1), 2-12.

ABSTRACT

Lithium-ion batteries have recently become the focus of research in vehicle applications due to their numerous advantages. Lithium-ion batteries have higher specific energy, better energy density, and a lower self-discharge rate than other secondary batteries, making them appropriate for electric vehicles and hybrid electric vehicles. Nonetheless, worries about safety, cost, charging time, and recycling have hampered the commercial usage of lithium-ion batteries for automotive applications. An accurate battery model on a simulation platform is required for the development of an effective battery system. In this study, a battery model is built in MATLAB/Simulink. Two variations are available: one with a series–parallel battery arrangement and a single model without configuration. The structure of the proposed model is provided and explained in detail. Based on the test results, the developed battery model was validated. A comparison shows that the model created can accurately predict current, voltage, and power performance. This model is designed for Eaton Electromechanical Battery Li-ion 18650 batteries but is also said to work with other types of batteries. The simulation takes into account the battery's state of charge, current, voltage, and power requirements.

Index Terms—Charge status, hybrid electric vehicles, lithium-ion battery, MATLAB/Simulink

I. INTRODUCTION

The energy factor is a vital component of the growth of any society [1]. Battery technology has advanced significantly in recent decades, particularly in lithium-ion batteries (LIBs) [2]. LIBs have dominated the market for advanced energy sources in today's society since they are widely employed in several industries such as electronics, electric vehicles (EVs), and energy storage systems [3]. A rechargeable battery may perform an electrochemical conversion, which means that the stored chemical energy can be turned directly into electric energy. In the system, chemical energy is transformed into electric energy during the charge and back to chemical energy during the discharge. Depending on the electrochemical system, this system may be charged and discharged more than 500 times. Because lithium-ion movement within the battery is followed by charge flow in an external circuit, the efficiency of lithium-ion movement in the electrolyte impacts the battery capacity [2]. Rechargeable batteries are important for future technologies because they have the potential to be employed as energy storage elements in green technology applications such as EVs and photovoltaic systems. Two traditional energy storage systems, such as batteries, have constraints such as slow charging and a limited lifespan [4]. LIBs, in particular, have become an essential component of decentralized, often tiny or micro-scale, off-grid renewable energy systems, supplanting diesel generators in many remote areas. LIBs are a potentially clean technology that can be utilized to replace typical fossil-fuel-powered gadgets. LIBs with better specific energy, low self-discharge, and improved coulombic efficiency are required for electric cars, railways, and spatial technologies [5].

Accurate battery information, such as state of charge (SOC), current, and voltage, is crucial for circuit designers to regulate the energy consumption of battery electrical systems. As a result, having a reliable battery model is critical for forecasting battery properties during the circuit design process. The SOC of LIBs indicates the remaining power of the battery [6]. It can be used to prevent the battery from being overcharged or overdischarged, predict the driving range of EVs, and eliminate the inconsistency of different cells. Furthermore, the estimation method is sensitive to factors like temperature, cycle

Received: September 28, 2023
Revision Requested: October 26, 2023
Last Revision Received: November 7, 2023
Accepted: November 10, 2023
Publication Date: January 3, 2024

Corresponding author: Azemtsop Manfo Theodore, azemsouleymane@yahoo.fr

time, discharge rate, voltage, and noise, making it difficult to correctly estimate the SOC of a battery in real time [7].

A comparable circuit model is commonly used by circuit designers since it can be easily performed in circuit simulators [8, 9]. To predict the current–voltage behavior of the batteries, the simulation models employ the MATLAB software curve-fitting toolbox, which connects the circuit model to the resistor–capacitor circuit [10]. A circuit version similar to the battery may be created within the MATLAB/Simulink environment to series the battery equations using differential equations that calculate the dynamics of the battery parameters [11-13].

The proposed LIB circuit model is built in MATLAB/Simulink in this study. Unlike the single-battery model, the recommended battery architecture's parameters vary based on SOC, current, voltage, and capacity, allowing the circuit designer to set the parameters primarily based on battery conductivity. Furthermore, the proposed version is without difficulty related to different MATLAB/Simulink circuit blocks, bearing in mind real-time SOC estimation. As a result, accurate SOC estimation is necessary to protect the battery and avoid overcharging and discharging. This will also help to prolong the life of the battery.

II. LITERATURE REVIEW

A. Electrochemical Storage Device

An electrochemical generator generates electrical energy directly from chemical energy. Batteries, accumulators, and fuel cells are the three types of electrochemical generators. The history of electrochemical generators begins in 1800, with Alessandro Volta's invention of the non-rechargeable primary cell [14].

Gaston Planté constructed the lead accumulator in 1859 after discovering the reversibility of electrical chemical reactions due to current reversal. It is composed of lead alloy grids that have been glued together with a mixture of sulfuric acid, lead oxide, and water as the active ingredient. This strategy enabled an electric car shaped like a torpedo to surpass 100 km/h in 1899 [15]. It was the first commercially available rechargeable battery. Lead-acid batteries are still utilized in automobiles for 12V and 15V power sources. The popularity of this type of battery can be attributed to the inexpensive cost of lead and sulfuric acid, ease of manufacture, and short lifespan [16].

Sony introduced the first lithium-ion rechargeable batteries in 1991 [17]. This technology quickly rises to prominence due to its specific energy, load capacity, and electromotive force performance. The nominal battery voltage in an LIB is 3.7 volts per cell. When an electrical device is linked to an LIB, the blocked electrons travel through the device and power it. An LIB cell can function as a power cell (which delivers a high current load for a short period) or an energy cell (which delivers sustained current for a long period of time). An LIB is made up of an anode, a cathode, an electrolyte, a separator, and a current collector [18]. Table I outlines the properties of these various battery technologies [14].

Main Points

- A new series/parallel lithium battery pack model was proposed using MATLAB/Simulink.
- The characteristics of the proposed battery model were simulated and analyzed.
- The discharging behavior in a single battery and the proposed pack model.
- The performance of the proposed model for application in electric vehicles and hybrid electric vehicles was compared and evaluated.

B. Classification of Lithium-Ion Batteries

The vocabulary used to describe LIB chemistry is denoted by shortened letters. The chemistry of cathode materials impacts the efficacy of an LIB. Cobalt has long been used as a component of LIBs. The difficult acquisition of expensive cobalt, on the other hand, calls into question its usefulness as a battery material. Battery manufacturers have been researching several types of LIBs to prevent risky sourcing methods while boosting cost, loading capabilities, and longevity. However, there are several types of LIBs, each with its own set of advantages, such as lithium manganese oxide, which has a high specific power; lithium cobalt oxide, which has high specific energy; lithium nickel cobalt aluminum (NCA) oxide and lithium nickel manganese oxide, which are the most thermally stable and cheapest; and lithium titanate oxide, which has a fast charge, a long life, but a higher cost and low specific energy [19]. The chemical composition of an LIB is crucial to its power, resilience, and safety in a variety of applications. Tesla, for example, uses a lithium-iron-phosphate battery chemistry for its standard-range vehicles and an NCA battery chemistry for its longer-range vehicles. Each battery performs differently and is chosen depending on the application [20]. Table II depicts commercial LIBs and their various features [21].

C. Battery Structure and Modeling

An LIB pack is composed of clusters of individual LIB cells that are organized in series and parallel, or both directions to generate the desired capacity, power density, or voltage for a variety of applications. A battery has an extremely short cycle life when exposed to dampness. As a result, it is vital to monitor moisture, cold temperatures, and increasing storage temperatures, as these factors can have a major impact on battery performance. A battery management system (BMS) is an electrical system that monitors individual cells within a battery pack to improve safety and performance.

LIBs do not refer to any specific device type. Instead, there are a variety of chemical and mechanical arrangements, each with its own set of features [22]. A BMS is required to properly employ a battery system in a real-world application. BMSs are used to monitor and control numerous cell states as well as to activate in the event of abuse or failure [23, 24]. In recent years, the development of control-oriented models has resulted in a plethora of modeling approaches that can be broadly characterized as electrochemical based models, equivalent circuit models, and data-driven models [25, 26].

With a better understanding of the battery's behavior, the next step in its management is the estimation of unmeasured internal

TABLE I.
COMPARISON OF SEVERAL BATTERY TECHNOLOGIES

Type	Electromotive Force in Volts	Number of Cycles	Charging Efficiency (%)	Gravimetric Energy Density (Wh/kg)	Volumetric Energy Density (Wh/L)	Temperature (°C)
Lead acid	2.1	500–1200	–	15–45	40–80	(–40)–40
Nickel-cadmium	1.2	≈2000	60	30–60	80	(–20)–60
Nickel metal hydride	1.2	500–1200	60	100	200	(–20)–60
Lithium polymer	3.7	≈1000	–	100–130	140–435	(–40)–40
Lithium ion	3.6	1000–10 000	95	150	300	(–20)–60

TABLE II.
LITHIUM-ION COMMERCIAL BATTERY COMPARISON

Abbreviation	LCO	LNO	LMO	NMC	LFP	NCA	LTO
Year	Since 1991	Since 1996	Since 1996	Sine 2008	Since 1993	Since 1999	Since 2008
Nominal voltage (*V*)	3.7~3.9	3.6~3.7	3.7~4.0	3.8~4.0	3.2~3.3	3.6~3.65	2.3~2.5
Specific energy (Wh/kg)	150~200	150~200	100~150	150~220	90~130	200~260	70~85
Charge (C)	0.7~1	0.7~1	0.7~1	0.7~1	1	0.7	1
Discharge (C)	1	1	1	1	1	1	10
Lifespan	500~1000	>300	300~700	1000~2000	1000~2000	500	3000~7000
Thermal runaway (°C)	150	150	250	210	270	150	–

LCO, lithium cobalt oxide; LFP, lithium-iron phosphate; LMO, lithium manganese oxide; LNO, lithium nickel dioxide; LTO, lithium titanate oxide; NCA, lithium nickel cobalt aluminum oxide; NMC, lithium nickel manganese.

variables. State of charge and state of health are critical cell parameters that cannot be directly quantified [27]. Battery parameters play an important role in battery management. While they change slowly (due to aging), learning more about them is desirable. While offline testing or open-loop calculation (for example, Coulomb counting for SOC calculation [28]) can provide an estimate, live closed-loop estimation of these indicators is crucial for robust and accurate real-time monitoring.

In the MATLAB graphical editor Simulink, a generic model of an LIB is built and validated (Fig. 1). It is portrayed as a controlled voltage source that is dependent on the SOC of the battery. The concept behind this design is to use a simple way to extract the input parameters for the battery model (shown in Fig. 2) from the battery manufacturer's catalog data. The model has different battery voltage dependency features depending on the operation modes.

III. LITHIUM-ION BATTERY MODEL

These days, the most common battery is LIB, which may be discovered in most transportable gadgets, starting from mobile telephones to laptops. Fig. 1 depicts a photo of this battery. LIBs have an extensive operational temperature range, as they can rate between –20°C and 60 °C and discharge between –40°C and 65 °C. LIB cells have a voltage of 2.5 to 4.2 *V*, which is about three times better than different styles of batteries [29–31].

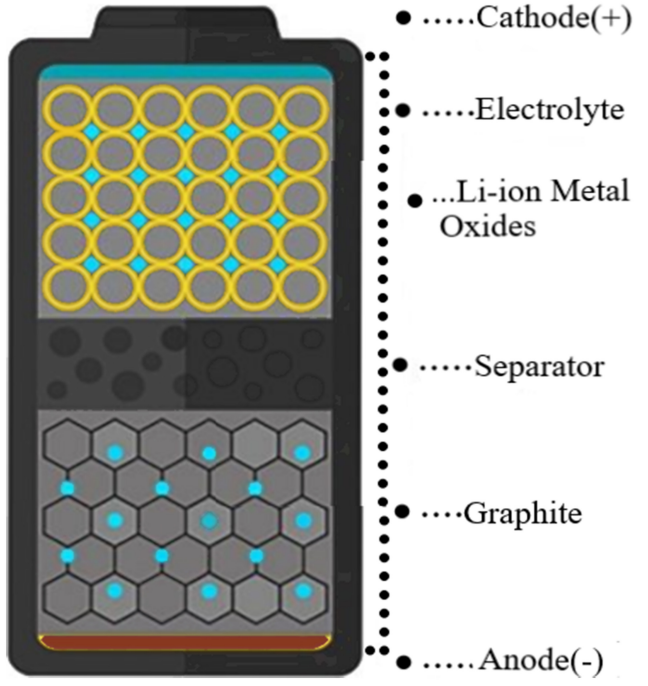

Fig. 1. Li-ion battery model [31].

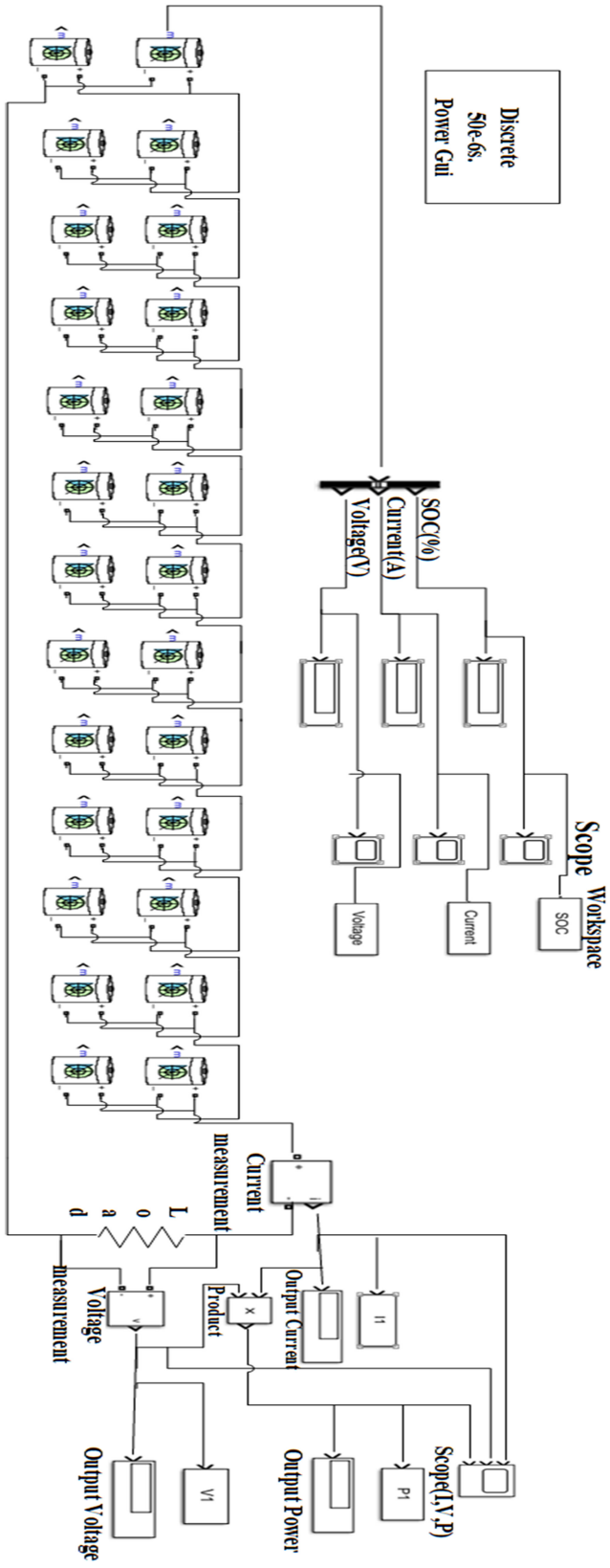

Fig. 2. Proposed model of series/parallel lithium-ion batteries packed model.

A. Mathematical Modeling of the Battery

This is accomplished by applying a mathematical battery model to calculate the open circuit voltage (OCV) of the battery and SOC parameters. Peukert's equation is one of the simplest mathematical equations for estimating the SOC of a battery. Peukert's rule was published in 1897 by the German physicist W. Peukert to define battery capacity variations throughout discharge time using Peukert's constant [32]. The capacity of a lead-acid battery is calculated using the rate of discharge [33]. The discharge curve of the battery in Fig. 3 is non-linear and is expressed by (1), where the charge current of the Shepherds model [34] is positive (i.e., >0):

$$f_1(i_t, i^*, i) = E_0 - K\frac{Q}{Q - i_t}.i^* - K\frac{Q}{Q - i_t}.i_t + Aexp\left(-B.i_t\right) \quad (1)$$

where E_0 is the constant voltage (V), K is the bias resistance (Ω), i^* is the low-frequency current dynamics (A), i_t is the battery current (A), Q is the maximum battery capacity (Ah), A is the exponential voltage, and B is the exponential capacity (Ah^{-1}).

The reverse discharge curve is depicted here (beginning with an empty battery, progressing to a quick rise to rated voltage after charging to rated voltage, and finally to the exponential area when the OCV is restored) (2):

$$f_1(i_t, i^*, i) = E_0 - K\frac{Q}{Q + 0.1i_t}.i^* - K\frac{Q}{Q - i_t}.i_t + Aexp\left(-B.i_t\right) \quad (2)$$

Because the load current has the opposite sign ($i^* < 0$), the bias resistance changes, and the function of the load voltage is slightly altered [35]. The effect of temperature on the LIB operation is not considered in this paper.

As the battery discharge curve in Fig. 3 shows, battery performance decreases as the discharge rate increases. The discharge rate ampere value is expressed as (3):

$$C_p = I^k t \quad (3)$$

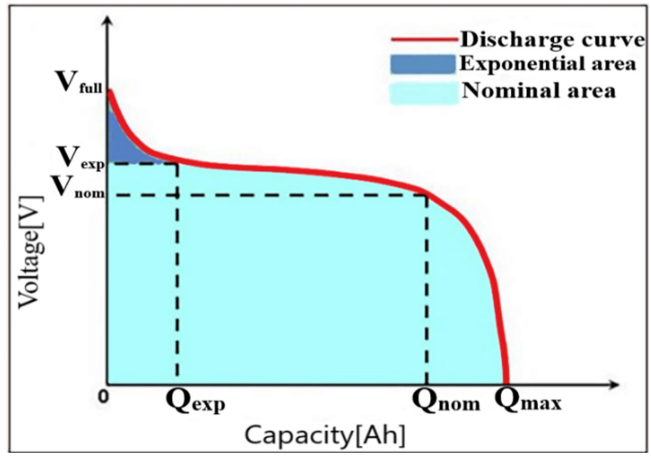

Fig. 3. Typical battery discharge curve.

where C_p is the capacity at a discharge rate of 1 amp (Ah), I is the current drawn by the load, and t is the time (h). Normally, the battery cell discharge rate is not 1 Ah. Changing the calculation formula according to the capacity and discharge amount gives (4):

$$C_p = H\left(\frac{C}{IH}\right)^k \tag{4}$$

In (4), the nominal discharge time in hours is H, the nominal power Ah at discharge rate is C, I is the measured discharge current, k is the Peukert constant, and t is the battery discharge time in hours [36].

IV. BATTERY DISCHARGE EXPERIMENTS

A. Voltage Versus Time

In EVs, the number of batteries is connected in a series-parallel configuration to meet the load requirement. Due to manufacturing methods, not all batteries reach maximum voltage at the same time during charging. This condition causes voltage imbalances between batteries and, as a result, lesser capacity from the entire battery string [37]. Generic batteries and their standards have undergone modifications to accommodate the specific requirements of different battery types and their charge and discharge characteristics. By utilizing the default properties of the battery model, we employed the draw option to visually depict the parameter values. An Eaton Electromechanical Battery (EEMB) Li-ion 18650 battery serves as the designated power source for reference purposes. The positive (+) and negative (–) terminals of the battery are utilized as buffer terminals, while multiple vector signals (m) [38] are employed as output terminals.

Fig. 4 presents the (Fig. 4a) block parameters and (Fig. 4b) typical discharge characteristics of an LIB. The features can be classified into three primary categories. The first category is the exponential range, which encompasses voltages exceeding the nominal value. The second category is the battery operating point, which refers to the period when the battery is inactive and generates a consistent discharge current.

In the nominal operating range of the battery, there is a slight variation in voltage during the discharge process. When the battery is scheduled for discharge, there is a third operational period in which the battery undergoes the process of discharging. The battery discharge curve, depicted by the blue line in Fig. 4, exhibits nonlinearity and is characterized by the Shepherd model [34]. The current flowing during the charging process is positive ($i^* > 0$). The polarization voltage, which can be determined by multiplying the series resistance by the battery current, serves as an indicator of the battery's discharge behavior. Fig. 4 illustrates the alterations in discharge characteristics resulting from variations in current.

In the voltage–time diagram, the current value of 5.4348 A represents the discharge characteristics observed during discharge at a constant current value. Additionally, the battery discharge was found to be correlated with currents of 0.52 C (6.5 A), 1.04 C (13 A), 2.08 C (26 A), and 4.16 C (52 A). The discharge duration is 2 h at a rate of 0.5 C and 15 min at 4 C. As a consequence, the battery's range experiences a notable decrease as the rate of current discharge rises.

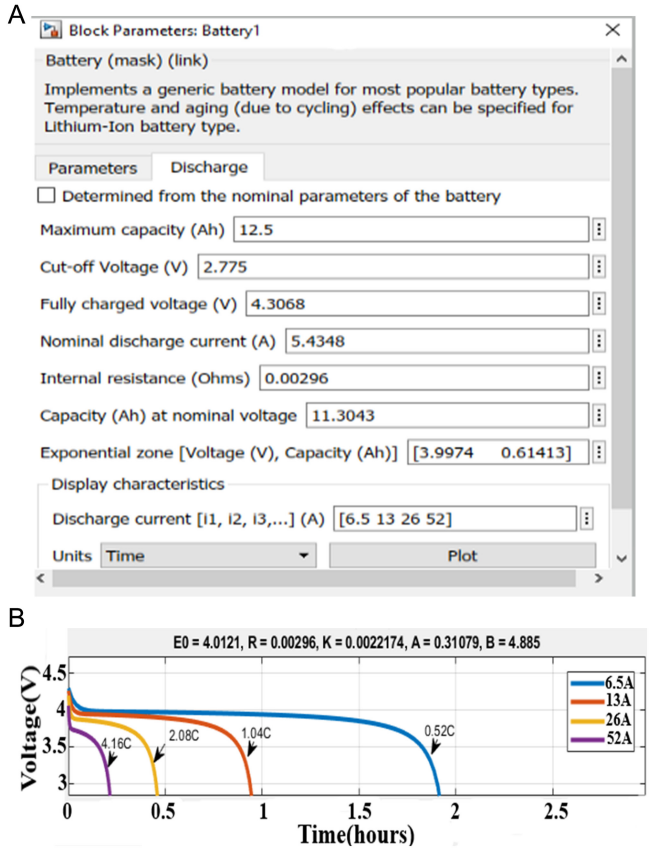

Fig. 4. (a) Block parameters and (b) battery discharge characteristics.

B. Battery Voltage Versus Discharge Capacity

The LIB model is stimulated with electrical aspects to estimate battery frequency at room temperature (RT). A continuous discharge test is performed on the battery with a constant current. Typical discharge curves for the EEMB Li-ion 18650 battery model operated at different discharge currents (6.5 A, 13 A, 26 A, and 52 A) are shown in Fig. 5. During battery testing, the battery voltage is set to a limit value (e.g., 2.775 V) defined by the battery manufacturer to avoid lasting damage to the battery.

A noticeable trend is observed wherein the discharge capacity diminishes with an increase in the applied current. The discharge curve exhibits a downward shift when the operating current is increased from 6.5 A to 52 A. According to the data presented in Fig. 5, the battery's full charge voltage at RT is recorded as 4.30 V. However, when the battery is discharged at various currents, the discharge capacity decreases to 52 A, resulting in a voltage drop of approximately 5% to 4.20 V. The development of a battery performance management system is highly significant in this context.

V. A GENERIC MODEL DISCHARGE AND CHARGE

The basic configuration of an LIB includes a current measurement connected to the battery's positive terminal, a load resistance (R) in parallel with a voltage measurement connected to the battery's negative terminal, and the battery circuit's internal resistance.

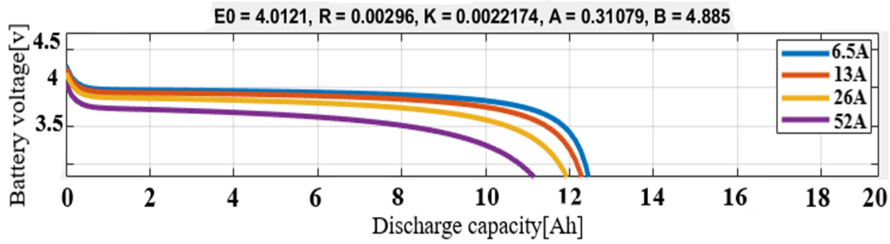

Fig. 5. Estimation of the battery voltage versus discharge capacity.

Resistance limits or regulates the current flow within the battery model to prevent overcharging. The output signal parameter is not used if the block is not used in pointer simulation. The simulating cursor is activated by a Powergui block set up in the model. The auto solver is not selected in the Simulink solver options to enable the Powergui solver. The simulation type, including simulation parameters and settings, is defined by the options menu block Portable Batch System.

In this study, MATLAB/Simulink is used to create a dynamic model of an EEMB Li-ion 18650 battery. Fig. 2 shows the overall dynamic model of a Simulink LIB. A fixed resistance constant was applied ($R = 1.1\ \Omega$), with a simulation time of 2000 s.

A. Current, Voltage, and Power Profile Comparison of Constant Current and Constant Power Discharge

Fig. 6 shows the discharge curves of the EEMB Li-ion 18650 battery pack model. The discharge curves of current, voltage, and power follow the same trend. Two regimes are observed in the three graphs: a drop and a relaxation regime. The internal resistance of the battery caused the voltage drop.

After the application of a constant resistance ($R = 1.1\Omega$), the battery model under investigation successfully supplied current to the battery pack connector. Fig. 6a-c depict the current, voltage, and power characteristics of the battery model during a 2000-s operation period. In Fig. 6a, it is evident that the current exhibits a gradual decline over time as the battery undergoes discharge, eventually reaching a stable state at $t = 1800$ s. This decrease in current is due to energy dissipation in the resistor, which generates heat and, as a result, reduces total current flow, stabilizing the system. In Fig. 6b, it can be observed that the voltage of a fully charged battery follows a similar trend as the discharge current, decreasing after surpassing the rated voltage until $t = 1800$ s. Given that the discharge and voltage curves exhibit a similar pattern, it is imperative to examine the power generated by the poles of the battery model while considering the impact of resistive effects.

The power curve exhibits a gradual decrease until it reaches $t = 1600$ s, at which point it becomes constant, as depicted in Fig. 6c. The power output at maximum charge was initially measured at 16.90 W but subsequently decreased to 14.5 W. The resistive effect of the system is responsible for controlling the spill current. Ohmic power loss exhibits an inverse relationship with resistance, as stated by relationship in (5).

$$P = V.I = RI^2 = V.\left(\frac{V}{R}\right) = \frac{V^2}{R} \tag{5}$$

where V is the supply voltage applied, I is the battery current, and R is the resistance.

The power output P of the battery pack model is calculated as follows.

$$P = P_{max} - RI^2 \tag{6}$$

where P_{max} corresponds to a maximum value of P in the battery model.

It is vital to note that the battery's power ranges between a peak of 16.90 W and a constant output of 14.50 W during both the charging and discharging processes. This indicates an approximate capacity fading of 14%. The conclusion is also influenced by the mechanical properties.

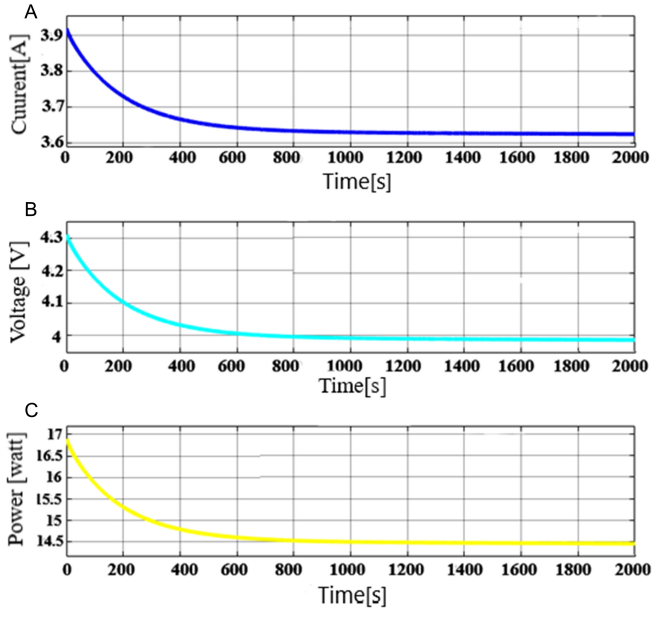

Fig. 6. (a) Current, (b) voltage, and (c) power profile comparison of constant current and constant power discharge.

TABLE III.
DIFFERENT SIMULATION PARAMETERS OF LI-ION BATTERY MODEL AND THEIR VALUES FOR DIFFERENT VALUES OF RESISTANCE

Resistance (Ohms)	State of Charge (%)	Output Current (A)	Output Voltage (*V*)	Power Delivered (W)
0.5	99.81	8.503	4.252	36.15
1	99.99	4.287	4.287	18.37
1.5	99.94	2.866	4.298	12.32
2	99.95	2.152	4.305	9.264
2.5	99.96	1.723	4.308	7.424
3	99.97	1.437	4.311	6.194
3.5	99.97	1.232	4.312	5.313

The determination of the energy expended by the battery throughout the charge/discharge cycle necessitates the integration of the power function with time. To ascertain the capacity of a battery pack to provide the desired energy at a particular voltage, Equation (7) is employed:

$$C = \frac{W}{3600.U} \tag{7}$$

where C is the capacity of the battery pack (Ah), W is the the total energy required for the charge/discharge cycles (J), and U is the nominal voltage of the battery pack (V).

When computing the energy of a simulated charge–discharge cycle, the sum of the power functions over time gives the total electrical energy stored in the battery ($W_{TOTAL} = 53.9$ kJ). LIBs have a capacity ranging from 25% to 95%, with only 70% of their theoretical capacity being safe to use. To obtain the right amount, divide the calculated total energy that the battery should give by (7) [39]. This suggests that the theoretical required battery capacity is around 5.78 Ah.

As shown in Table III, power output decreases as load resistance increases. If the load resistance drops too much, the voltage across the internal resistance of the power supply will drop significantly, greatly impacting performance. However, the initial charging state was reached when the load resistance was 1Ω.

VI. PROPOSED BATTERY PACK CONFIGURATION

Battery pack references find application in numerous scenarios that involve series and parallel cell configurations. Parallel connections have the effect of increasing battery capacity, while series connections have the effect of increasing battery voltage. Fig. 2 illustrates the battery model that is recommended, which is based on a configuration of 26 cells. Thirteen series Li-ion 18650 batteries are arranged in a configuration where 13 parallel Li-ion 18650 batteries are combined to create a battery pack model.

A. Validation of Battery Pack Model

In the present study, a Li-ion 18650 battery manufactured by EEMB was utilized as the battery model. This particular battery has a nominal voltage of 3.7 V and a capacity of 11.30 Ah. In this study, the parameters are extracted from a previous study [39], in which the resulting experiment demonstrated that the percentage error from the nominal voltage was below 2%. The battery pack model proposed in this study is subsequently validated through a series–parallel arrangement of battery cells. The battery pack model suggested in this study is then validated using a series–parallel configuration of battery cells. The battery pack model is used to compare simulation results to the previously reported simulation findings for the single-battery model.

B. State of Charge (%) Versus Time

The SOC of a cell indicates the amount of its current capacity compared to its nominal capacity. Fig. 7 illustrates the SOC graph for both the single-battery and pack-battery models. It can be observed that the SOC of the single battery shows a straight line indicating its quick discharge, as seen in Fig. 7a, and the SOC graph for the battery pack model gradually discharges from the fully charged state to the steady state at $T = 10$ s, as seen in Fig. 7b. In this simulation, the thermal and mechanical impacts on the storage system are not considered. The SOC of the single-battery model was 89.33% and 93.99% for the pack-battery model after applying a load of 0.005 Ω. The simulation of the proposed configurations demonstrates that

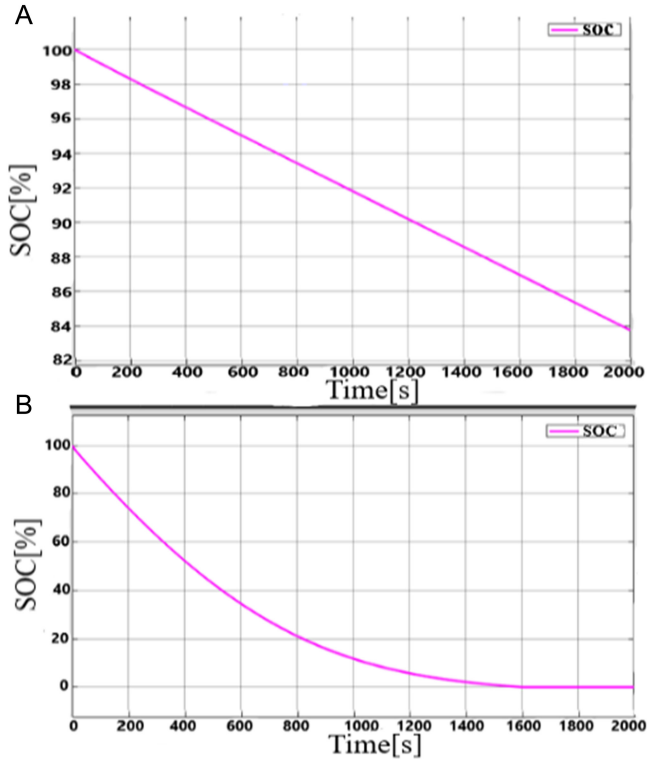

Fig. 7. (a) SOC vs. time curve for the single-battery model and (b) proposed battery pack model. SOC, state of charge.

the discharge rate is lower compared to that of the single-battery model. This statement signifies the augmentation of its capacity. The battery cell assembly exhibits a discharge rate of 85.54 A, which is nearly twice the standard value of 42.77 A for the battery model, owing to its parallel configuration. In the context of battery systems, when configured in series, there is no substantial difference in SOC between the battery model and the series–parallel setups. The battery pack model simulates SOC with great accuracy, as the observed inaccuracy is small.

This result was similar to that found by Bhagat et al [20] in their proposed circuit for discharging LIB. They used three Li-ion cells (each 12 *V* and 6 Ah) connected in series and adapted the nominal voltage, rated capacity, and SOC to their needs. A load resistance was added, and resistance value was set. A metal-oxide-semiconductor field-effect transistor (MOSFET) (to control the circuit) and the current measurement were inserted. A scope and a display were added that showed current readings. The MOSFET was connected to the first battery, and the resistance was connected to the third battery. Thus, the MOSFET was used as an adjustable resistance. A bus selector was finally connected to the first battery; the selection in the bus chooses SOC, current, and voltage. Another scope was inserted to show the waveforms, and the SOC signal was connected as input to the relational operator. The SOC signal was used as an input for the relational operator. As a result, when SOC equals zero, the relation operator outputs a low signal. Voltage measurement connected its two ends to the positive and negative ends of the battery, further adding a scope and display to it, including a display of the SOC value. Although the voltage and current initially fell but eventually remained constant across the duration, the battery's SOC reduced over time.

The results also showed how battery 3 (12V and 6Ah) and channel lining evolved. As we can see in this model, the battery's SOC decreases with time, and the voltage and current initially decrease but then follow a steady pattern throughout the period. The channel lining remains unaltered during the run.

C. Comparison of State of Charge in a Battery Model and Battery Pack Model

The OCV curve was defined in our study as the mean value of the charge and discharge equilibrium potentials. OCV is the terminal voltage of the battery in an equilibrium state [40]. The effect of hysteresis was overlooked. Furthermore, as stated by reference [41], the OCV–SOC curve is found to be unique for the same type of cell under the same testing conditions. Fig. 8 illustrates the mean OCV at 25°C. A relatively level gradient ranging from 94% to 95% SOC is emphasized in both graphs. The pack model exhibits a significant increase in comparison to that of a single battery. This observation emphasizes the variations in OCV–SOC curves within the range of 93%–100% SOC at ambient temperatures. It is logical to conclude that the discharge capacity of a single-battery model decreases significantly, dropping as much as 95% before stabilizing. Firstly, the battery pack underwent a complete charging process with a continuous current of 1 C. The 1 C rate signifies that the battery would take approximately 1 h to discharge completely. The charging process continued until the voltage reached the cutoff value of 5.93 V. The initial value of the

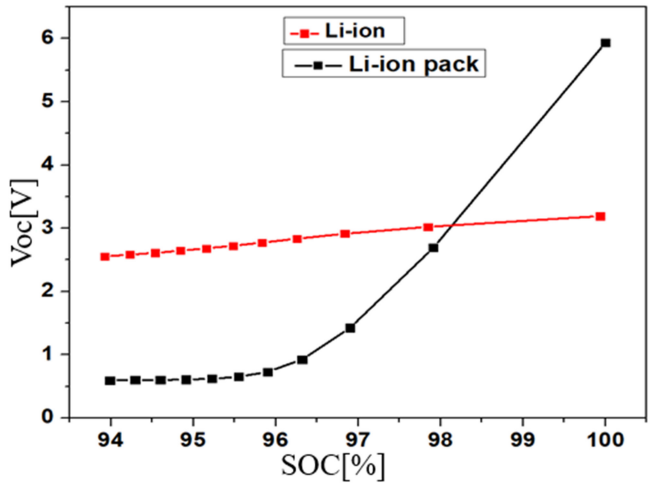

Fig. 8. V_{oc}–SOC curves of the single Li-ion battery and the battery pack model obtained at RT. SOC, state of charge.

battery pack is roughly double that of a single battery, and the current and voltage levels remain relatively consistent during the charge and discharge operation. The simulation parameters for the OCV and SOC values obtained for the single Li-ion and Li-ion pack models are in Table IV.

Fig. 8 shows the variation of the mean OVC with the SOC for the single Li-ion battery and the battery pack model obtained at 25°C. It is noteworthy that the battery model will experience depletion before reaching its rated voltage. The SOC curve of the lithium-ion pack model was consistently found to be associated with the SOC curve of the battery model. A single battery exhibits a highly linear

TABLE IV.
THE SIMULATION PARAMETERS OF THE V_{OC} AND SOC OBTAINED FOR THE SINGLE LI-ION AND LI-ION PACK MODEL

Lithium-ion battery		Lithium-Ion Battery Pack	
Open Circuit Voltage	**State of Charge(%)**	**Open Circuit Voltage**	**State of Charge(%)**
2.71538	100	5.93802	100
2.54546	97.91188	2.69218	97.91188
2.43682	96.90312	1.42368	96.90312
2.35896	96.319	0.92402	96.319
2.24854	95.90193	0.72764	95.90193
2.20602	95.55058	0.65018	95.55058
2.20602	95.22529	0.61915	95.22529
2.1689	94.91059	0.60618	94.91059
2.13601	94.60049	0.60021	94.600049
2.10658	94.29265	0.59694	94.29265
2.08008	93.98618	0.5947	93.98618

curve, which enables an accurate evaluation of its SOC. The SOC can be pretty accurately approximated using the observed voltage. We can see that SOC is a superior statistic to voltage for determining how full a specific battery is. This must be considered while designing a system, identifying batteries, and using them.

The LIB pack, on the other hand, exhibits a relatively flat discharge curve, indicating that the voltage at the battery terminals experiences only minimal fluctuations over a wide range of operating conditions. The battery input values were utilized to validate the proposed model in MATLAB, as depicted in Fig. 8.

D. Current, Voltage, and Power Profile Comparison of Constant Current and Constant Power Discharge

The discharge test depicted in Fig. 9 demonstrates that the output parameters of the proposed battery cell model are higher than those achieved with the single-battery model.

Fig. 9a illustrates the observed behavior of the battery model upon battery drain. The battery cell design was charged to 100% SOC using the constant current, constant voltage method. Subsequently, it was discharged to 0% SOC with a constant current of 1 C. This period is characterized by the cessation of current flow after discharge, and the battery voltage gradually reaches a steady state. The battery cell model demonstrates a discharge in forced mode until $t = 1600$ s, followed by a transition to relaxed mode. During the idle phase, the processes of polarization and material exchange within the battery exhibit sluggishness, resulting in voltage fluctuations. In comparison to the battery of the conventional model, it was observed that the maximum current value (I) reached 42.77 A and the maximum voltage measured was 94 V. These values were found to be higher than those of a single battery, indicating an increased capacity.

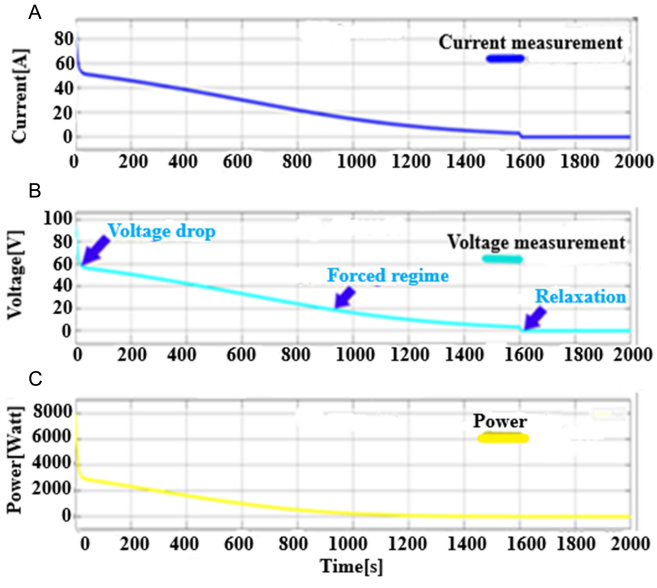

Fig. 9. (a) Current, (b) voltage, and (c) power discharge profile comparison of constant current and constant power discharge.

The depiction of the second stage of battery voltage can also be observed in Fig. 9b. A phase drop is observed when there is a change in the current level. Another factor to consider is the duration of the forced regime period during which the battery current does not reach zero ($t = 1600$ s). This result was also similar to that of the discharging circuit of the Li-ion model proposed by Bagh and his team [20] when they studied the variation of current, voltage, and SOC against time. They discovered that the individual variation of the SOC, voltage, and current of a 12V and 6 Ah battery reduced linearly with time. The voltage originally increased from 14 V to 13.8 V at t = 0, then began declining parabolically until time t = 270 s, and remained steady until the conclusion. Likely, in this scenario, the current increased from 0 to 85.54 A at t = 0, then began to decrease until t = 1600 s, and remained constant over the entire duration.

The battery model is first charged to a specific current of $I = 85.54$ A and a voltage of 94.10 V. It is then discharged in a forced mode until the relaxation time is achieved at $t = 1600$ s. The system consistently provided a power output of 8049 watts, as depicted in Fig. 9c. By comparison, the previous battery model had a capacity of 16.85 W and was discharged until reaching 0 V. However, the voltage during discharge decreases due to the internal resistance of the cell. During the process of power discharge, the voltage of the cell remained consistently at 36.02 V, leading to a corresponding current value of 30.44 A. The calculation of the total energy consumption following complete discharge yields a value of $W_{TOTAL} = 16.12$ MJ, which is three orders of magnitude greater than the 53.9 KJ estimated in the battery pack. The pack model exhibited a capacity of 17.28 mAh.

E. Instantaneous Discharge Power Versus State of Charge

The discharge performance was assessed in the proposed model, with the SOC being considered a variable. This evaluation is depicted in Fig. 10. In the present study, the resistance of the battery (R_{batt}) and the battery's SOC are considered variables dependent on the temperature. The assumption is made that the battery temperature remains constant at 20°C and any potential temperature effects are disregarded.

The instantaneous current capacity of the battery pack is depicted in Fig. 10. The text provides a characterization of battery models utilized in electrical systems, specifically in the context of hybrid electric vehicles (HEVs). Standard experimental procedures were accessible within the advisor software utilized to generate the SOC chart data for the batteries employed. The proposed battery design demonstrates applicability despite the individual battery cell having a mass of 38 g and a nominal voltage of 3.7 V. This is due to its ability to be discharged up to 88 times, with a charge–discharge efficiency of 80%–90% for LIBs.

The performance of the battery model has exhibited significant improvement compared to the conventional model. A twofold increase in current output and a thirteenfold increase in voltage output were observed as a result of employing the 13-parallel and 13-series battery configurations, respectively. The battery pack model demonstrated exceptional electrical performance at ambient temperatures, surpassing that of a single battery with better SOC stability after a long discharge process. The observed characteristics

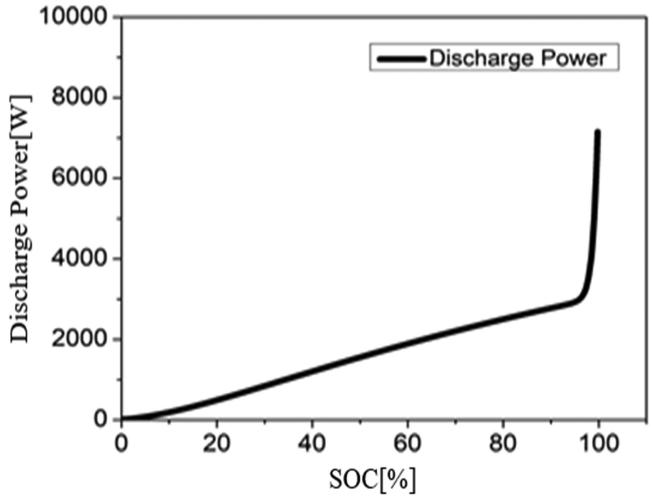

Fig. 10. Instantaneous discharge power versus SOC. SOC, state of charge.

of current, voltage, and power discharge demonstrate the anticipated enhancement in the performance of the proposed battery cell model, indicating its potential applicability to various battery types.

In this paper, the temperature effect is neglected. Taking the temperature effect into account necessitates the modeling effort mentioned in [42]. Using a 3D lookup table, the temperature effect can be included with a few adjustments.

VII. CONCLUSION

In this paper, it is aimed to provide guidance and simulate a model of the EEMB Li-ion 18650 battery pack. The battery model proposed in this study is configured in a series–parallel arrangement, allowing for the simulation of various discharge currents and the assessment of their impact on battery performance. Additionally, the model can estimate the battery's SOC and output power. The SOC of a series–parallel Li-ion battery is modeled and simulated using the MATLAB/Simulink tool. State of charge is investigated to determine the discharging behavior of a Li-ion battery pack. When a load is supplied to the battery, the performance of the suggested model, which includes SOC, current, voltage, and power, is evaluated. Modeling and simulating the circuit with set charge and discharge percentages aids in improving battery life and battery degradation, as shown in the battery circuit, has an SOC (%) that remains relatively constant with varying loads, indicating the model's stability at ambient temperature (Table III). The proposed model outperforms the single-battery model significantly. This study aims to contribute to the analysis of HEV battery capacity by predicting the discharge characteristics at various battery capacities. The simulation results demonstrate a strong resemblance between the proposed simulation model and the recorded test results from the battery data.

Peer-review: Externally peer-reviewed.

Author Contributions: Concept – T.A.M.; Design – T.A.M.; Supervision – Ş.M.E.; Ressources – T.A.M., Ş.M.E.; Materials – T.A.M., Ş.M.E.; Analysis and/or Interpretation – T.A.M.; Literature search – T.A.M., Ş.M.E.; Writing – T.A.M.; Critical Review – Ş.M.E.

Declaration of Interests: The authors have no conflict of interest to declare.

Funding: This research received no funding.

REFERENCES

1. A. M. Theodore, S. Konwar, P. K. Singh, R. M. Mehra, Y. Kumar, and M. Gupta, "PEO + NaSCN and ionic liquid-based polymer electrolyte for supercapacitor," *Mater. Today Proc.*, vol. 34, no. 3, pp. 802–812, 2021.
2. N. Badi *et al.*, "The impact of polymer electrolyte properties on lithium-ion batteries," *Polymers*, vol. 14, no. 15, pp. 3101, 2022. [CrossRef]
3. "N. Badi, A. M. Theodore, A. Roy, S. A. Alghamdi, A. O. M. Alzahrani, and A. Ignatiev, "Preparation and characterization of 3D porous silicon anode material for lithium-ion battery application," *Int. J. Electrochem. Sci.*, vol.17, no. 6, pp. 22064, 2022. [CrossRef]
4. A. M. Theodore, "Progress into lithium-ion battery research," *J. Chem. Res.*, vol.47, no.3, pp. 1–9, 2023. [CrossRef]
5. A. M. Theodore, "Promising cathode materials for rechargeable lithium-ion batteries: A review," *JSE*, vol. 14, no. 1, pp. 51–58, 2023.
6. S. Wang, C. Lu, C. Liu, Y. Zhou, J. Bi, and X. Zhao, "Understanding the energy consumption of battery electric buses in urban public transport systems," *Sustainability*, vol. 12, no. 23, pp. 10007, 2020. [CrossRef]
7. X. Y. Mao, "*Research on Li-ion Battery State of Charge and Active Equalization Technology*," Master's Thesis. Nanjing, China: Nanjing Univ. Posts Telecommun., 2020.
8. M. Chen, and G. A. Rincon-Mora, "Accurate electrical battery model capable of predicting runtime and I-V performance," *IEEE Trans. Energy Convers.*, vol. 21, no. 2, pp. 504–511, 2006. [CrossRef]
9. C. Liao, H. Li, and L. Wang, "A dynamic equivalent circuit model of LiFePO4 cathode material for lithium-ion batteries on hybrid electric vehicles," IEEE Vehicle Power and Propulsion Conference, 2009, pp. 1662–1665. [CrossRef]
10. W. Y. Low, J. A. Aziz, N. R. N. Idris, and R. Saidur, "Electrical model to predict current-voltage behaviors of lithium ferro phosphate batteries using a transient response correction method," *J. Power Sources*, vol. 221, pp. 201–209, 2013. [CrossRef]
11. M. C. Knauff, C. J. Dafis, D. Niebur, H. G. Kwatny, C. O. Nwankpa, and J. Metzer, "Simulink model for hybrid power system test-bed," IEEE Electric Ship Technologies Symposium, Arlington, VA, USA, 2007, pp. 421–427. [CrossRef]
12. "K. Yusuf, A. Ö. İlker, and S. İsmail, "Estimation of li-ion battery state of charge using adaptive neural fuzzy inference system (ANFIS)," *IJEAT*, Vol. 7, no. 3, 2020, pp. 88–94.
13. A. Afzal, R. K. Abdul Razak, A. D. Mohammed Samee, R. Kumar, Ü. Ağbulut, and S. G. Park, "A critical review on renewable battery thermal management system using heat pipes," *J. Therm. Anal. Calorim.*, vol. 2, pp. 1–40, 2023. [CrossRef]
14. K. Jaouad, B. Najib, and S. Abdallah, "Review on lithium-Ion battery modeling for different applications," *IJEAP*, vol. 1, no. 1, pp. 38–47, 2021.
15. M. Urbain, "*Modélisation Électrique et Énergétique des Accumulateurs Li-Ion. Estimation en Ligne de la SOC et de la SOH*," Thèse de doctorat. Institut National Polytechnique de Lorraine, 2009.
16. F. Miomandre, S. Sadki, P. Audebert, and R. Méallet-Renault, "*Électrochimie - 2e éd.:Des concepts aux applications*," Dunod, 2011. Available: https://books.google.com.tr/books?id=zis0_5G_x4sC
17. A. Eddahech, *Modélisation du vieillissement et détermination de l'état de santé de batteries lithium-ion pour application véhicule électrique et hybride*, Université Sciences et Technologies - Bordeaux I, 2013. Français. (NNT: 2013BOR14992). (tel-00957678)

18. S. Mahmud *et al.*, "Recent advances in lithium-ion battery materials for improved electrochemical performance: A review," *Results Eng.*, vol. 15, pp. 100472, 2022. [CrossRef]
19. L. Ianniciello, P. H. Biwolé, and P. Achard, "Electric vehicle batteries thermal management systems employing phase change materials," *J. Power Sources*, vol. 378, pp. 383–403, 2018. [CrossRef]
20. S. Bhagat *et al.*, *"Simulation of Li-ion Battery using MATLAB Simulink for Charging and Discharging*,"E3S Web of Conferences 353, 03001, EVF'2021, 2022.
21. Q. Wang, B. Jiang, B. Li, and Y. Yan, "A critical review of thermal management models and solutions of lithium-ion batteries for the development of pure electric vehicles," *Renew. Sustain. Energy Rev.*, vol. 64, pp. 106–128, 2016. [CrossRef]
22. Y. Miao, P. Hynan, A. von Jouanne, and A. Yokochi, " Current li-ion battery technologies in electric vehicles and opportunities for advancements," *Energies*, vol. 12, no. 6, pp. 1074, 2019. [CrossRef]
23. M. A. Hannan, M. S. H. Lipu, A. Hussain, and A. Mohamed, "A review of lithium-ion battery state of charge estimation and management system in electric vehicle applications: Challenges and recommendations," *Renew. Sustain. Energy Rev.*, vol. 78, pp. 834–854, 2017. [CrossRef]
24. S. B. Lee, R. S. Thiagarajan, V. R. Subramanian, and S. Onori, "Advanced battery management systems: Modeling and numerical simulation for control," Proceedings of the 2022 American Control Conference (ACCC), Atlanta, GA, USA, 8–10 June, 2022, pp. 4403–4414, 2022. [CrossRef]
25. U. Krewer, F. Röder, E. Harinath, R. D. Braatz, B. Bedürftig, and R. Findeisen, "Review—Dynamic models of li-ion batteries for diagnosis and operation: A review and perspective," *J. Electrochem. Soc.*, vol. 165, no. 16, pp. A3656–A3673, 2018. [CrossRef]
26. F. Brosa *et al.*, "A continuum of physics-based lithium-ion battery models reviewed," *Prog. Energy*, vol. 4, no. 04, 2003.
27. M. Martí-Florences, A. Cecilia, and R. Costa-Castelló, "Modelling and estimation in lithium-ion batteries: A literature review, *Martí-Florences, A. Cecilia, R, Energies*, Vol.16, no.19, 2023, pp. 6846.
28. K. Movassagh, A. Raihan, B. Balasingam, and K. Pattipati, "A critical look at coulomb counting approach for state of charge estimation in batteries," *Energies*, vol. 14, no. 14, pp. 4074, 2021. [CrossRef]
29. P. Singh, and D. Reisner, "Fuzzy logic-based state-of-health determination of lead-acid batteries," 24th Annual International Telecommunications Energy Conference, Montreal, QC, Canada, 2002, pp. 583–590. [CrossRef]
30. T. Huria, M. Ceraolo, J. Gazzarri, and R. Jackey, "High fidelity electrical model with thermal dependence for characterization and simulation of high-power lithium battery cells," IEEE International Electric Vehicle Conference, Greenville, SC, USA, Vol. 2012, 2012, pp. 1–8. [CrossRef]
31. A. J. Salkind, C. Fennie, P. Singh, T. Atwater, and D. E. Reisner, "Determination of state-of-charge and state-of-health of batteries by fuzzy logic methodology," *J. Power Sources*, vol.80, no.1–2, pp. 293–300, July 1999. [CrossRef]
32. L. David, and B. R. Thomas, *Handbook of Batteries*, 3rd ed., 1995.
33. G. Marcia, "*A battery's guide to immortality*," 2019. Accessed: 08 August 2019. Available: https://www.mtu.edu/magazine/research/2019/stories/ battery-immortality/
34. H. Xuebing, O. Minggao, and L. Languang, "A comparative study of commercial lithium-ion battery cycle life in the electrical vehicle: Aging mechanism identification," *J. Power Sources*, vol. 251, pp. 38–54, 2014. [CrossRef].
35. Available: https://www.mathworks.com/help/physmod/sps/powersys/ref/battery.html.
36. O. Tremblay, and L. A. Dessaint, "Experimental validation of a battery dynamic model for EV applications," *World Electr. Veh. J.*, vol. 3, no.2, pp. 289–298, 2009. [CrossRef]
37. K. W. E. Cheng, B. P. Divakar, H. Wu, K. Ding, and H. F. Ho, "Battery-Management System (BMS) and SOC development for electrical vehicles," *IEEE Trans. Veh. Technol.*, vol. 60, no. 1, pp. 76–88, Jan. 2011. [CrossRef]
38. D. Shen, L. Wu, G. Kang, Y. Guan, and Z. Peng, "A novel online method for predicting the remaining useful life of lithium-ion batteries considering random variable discharge current," *Energy*, vol. 218, pp. 119490, 2021. [CrossRef]
39. I. Husain, "Electric and hybrid vehicles: Design fundamentals," *Front Cover. CRC Press, - Technology & Engineering*, pp. 288, 2003.
40. L. W. Yao, J. A. Aziz, P. Y. Kong, and N. R. N. Idris, "Modeling of lithium-ion battery using MATLAB / Simulink," *IECON*, vol. 2013, pp. 1729–1734, 2013. [CrossRef]
41. H. Dai, X. Wei, Z. Sun, J. Wang, and W. Gu, "Online cell SOC estimation of Li-ion battery packs using a dual time-scale Kalman filtering for EV applications," *Appl. Energy*, vol. 95, pp. 227–237, 2012. [CrossRef]
42. L. Long, P. Bauer, and E. Kelder, "A practical circuit-based model for Li-ion battery cells in electric vehicle applications," IEEE Telecommunications Energy Conference (INTELEC), 2011, pp. 1–9. [CrossRef]